View metadata, citation and similar papers at core.ac.uk
brought to you by CORE
provided by Repositorio da Producao Cientifica e Intelectual da Unicamp

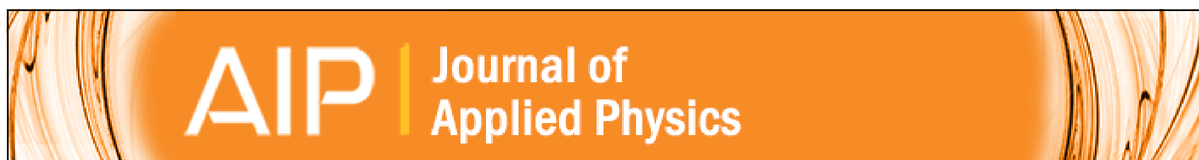


# Electrical characterization of epitaxial layers of In0.71Ga0.29As0.63P0.37

S. M. Shibli and M. M. Garcia de Carvalho

Citation: Journal of Applied Physics **64**, 235 (1988); doi: 10.1063/1.341469
View online: http://dx.doi.org/10.1063/1.341469
View Table of Contents: http://scitation.aip.org/content/aip/journal/jap/64/1?ver=pdfcov
Published by the AIP Publishing

**Articles you may be interested in**

Investigation of interfaces in AlSb/InAs/Ga0.71In0.29Sb quantum wells by photoluminescence
J. Appl. Phys. **116**, 123107 (2014); 10.1063/1.4896553

Photoemission characteristics of (Cs, O) activation exponential-doping Ga0.37Al0.63As photocathodes
J. Appl. Phys. **113**, 213105 (2013); 10.1063/1.4808291

Large magnetocaloric effect in single crystal Pr 0.63 Sr 0.37 Mn O 3
J. Appl. Phys. **97**, 10M306 (2005); 10.1063/1.1849554

Evidence for the occupation of DX centers in In0.29Al0.71As
J. Vac. Sci. Technol. B **14**, 2944 (1996); 10.1116/1.588939

Photoluminescence studies of the effects of interruption during the growth of single GaAs/Al0.37Ga0.63As quantum wells
Appl. Phys. Lett. **49**, 1245 (1986); 10.1063/1.97427

[This article is copyrighted as indicated in the article. Reuse of AIP content is subject to the terms at: http://scitation.aip.org/termsconditions. Downloaded to ] IP: 143.106.108.133 On: Tue, 25 Nov 2014 18:41:19

# Electrical characterization of epitaxial layers of $In_{0.71}Ga_{0.29}As_{0.63}P_{0.37}$

S. M. Shibli and M. M. Garcia de Carvalho
*Instituto de Física "Gleb Wataghin"-LPD/UNICAMP, 13081-Campinas/SP, Brazil*

(Received 19 November 1987; accepted for publication 9 March 1988)

We have performed measurements of carrier concentration and Hall mobility, between 4.2 K and room temperature, in InGaAsP (energy gap of 0.96 eV) epitaxial layers grown on semi-insulating InP. It is shown that for this kind of material in the range of concentration studied ($2.0\times10^{16}$–$1.6\times10^{18}$ cm$^{-3}$), alloy scattering has to be taken into account as a mechanism limiting the mobility even at low temperatures. Also, in the entire range of temperature and concentration studied, Fermi-Dirac statistics are better suited than Boltzmann statistics for theoretical calculations of Fermi energy, because even for concentrations as low as $2.0\times10^{16}$ cm$^{-3}$, the material is degenerated at low temperatures. Following these assumptions, we have calculated the alloy scattering potential as being between 0.52 and 0.62 eV.

## I. INTRODUCTION

The quaternary alloy $In_{1-x}Ga_xAs_yP_{1-y}$ can be epitaxially grown lattice matched to InP substrates. It has attracted great interest as a material for the fabrication of optoelectronic devices in optical-fiber communication systems.[1-3] The successful fabrication of double heterojunction lasers, avalanche photodetectors, etc., has already been reported.

In the electrical characterization of such materials, alloy scattering should be taken into account for mobility determination as demonstrated elsewhere.[4,5] Three theories have been used by most authors to explain this kind of scattering. The first attributes the scattering potential to the band-gap discontinuity (BGD) of the components of the alloy.[5-8] The second and third attribute the scattering potential to the electron affinities discontinuity (EAD)[9-11] and electronegativities discontinuity (END),[12] respectively. Analysis of experimental results and fitting with theory has to be done accurately in order to enable us to reach conclusions that permit us to distinguish among the different theories.

In this paper, we report measurements of electrical transport coefficients of $In_{0.71}Ga_{0.29}As_{0.63}P_{0.37}$ [energy gap $(E_g) = 0.96$ eV] between 4.2 K and room temperature. Similar measurements on the $In_{1-x}Ga_xAs_yP_{1-y}$ alloys have been performed by Bhattacharya *et al.*[13] between 20 K and room temperature and Greene *et al.*[14] between 77 K and room temperature. However, as we show in this work, the correct statistics have to be used in the data analysis. Thus, we used Fermi-Dirac statistics and with the mobilities measured at 4.2 K where the ionized impurity scattering is dominant, we can directly determine the total ionized impurity concentration for doped samples.

## II. EXPERIMENTAL PROCEDURE

Hall measurements were performed on epitaxial layers grown by liquid phase epitaxy (LPE) on Fe-doped semi-insulating InP. The layers are tin doped with a doping concentration between $2.0\times10^{16}$ and $1.8\times10^{18}$ cm$^{-3}$ and a typical thickness ($d$) around 0.5 $\mu$m.

The magnetic field used to perform Hall measurements is always 0.2 T. Ohmic contacts were obtained with conventional Au-Ge-Ni alloy. The four ohmic contacts were located, one each, at the middle of the four edges of the sample and only samples which presented good electrical symmetry were analyzed.

Samples were mounted in a cryostat in order to perform the measurements between 4.2 and 300 K. The temperature was measured with a Cryogenic Linear Temperature Sensor (CLTS), which was located in contact with the sample. The sensor was calibrated at three points: 4.2, 77, and 300 K. Thus, with two straight lines, one between 4.2 and 77 K and

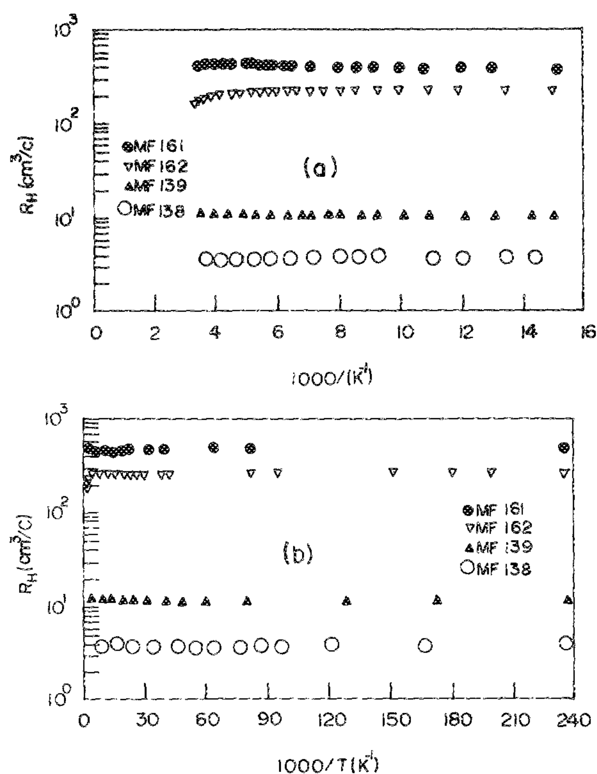


FIG. 1. (a) Hall constant vs $10^3/T$ between 65 K and room temperature. (b) Hall constant vs $10^3/T$ between 4.2 K and room temperature.

 0021-8979/88/130235-04$02.40 © 1988 American Institute of Physics 

[This article is copyrighted as indicated in the article. Reuse of AIP content is subject to the terms at: http://scitation.aip.org/termsconditions. Downloaded to ] IP: 143.106.108.133 On: Tue, 25 Nov 2014 18:41:19

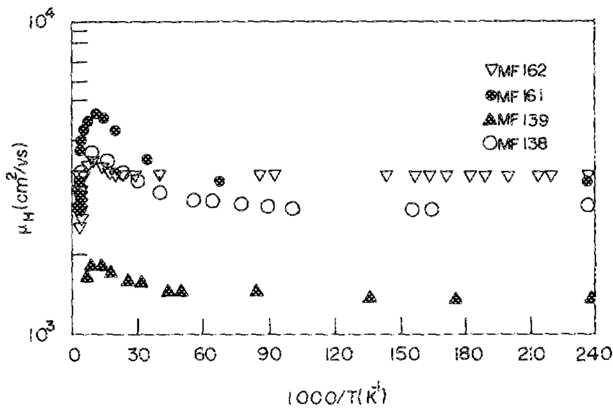


FIG. 2. Hall mobility vs $10^3/T$ between 4.2 K and room temperature.

another between 77 and 300 K, we were able to have a maximum temperature error of less than 1 K, following the vendor specification (Micro-Measurements).

Figures 1 and 2 show, respectively, the experimental variations of Hall coefficient ($R_h$) and Hall mobility ($\mu_h$) for all samples as a function of reciprocal absolute temperature. There is a maximum in the mobility around 150 K, which is caused by a change in the predominant scattering mechanism.

The curves of Fig. 1 show that carrier concentration ($n \sim 1/R_h$) is constant, in the range of temperatures studied, for the samples MF 138 and 139. Also, for temperatures lower than 50 K the remaining samples show the same behavior.

Table I summarizes some properties of the samples investigated and the experimental results obtained.

## III. ANALYSIS

Generally, the electron mobility in a polar semiconductor around room temperature is limited by carrier scattering due to phonons, ionized impurities, and random local fluctuations in the alloy composition. We calculated the electron mobility assuming the validity of Matthiessen's rule.[15] So, we assume that the important carrier scattering mechanisms are mutually independent and the total mobility can be obtained in the relaxation time approximation, from an arithmetic sum of the reciprocal mobilities calculated for each scattering event:

$$\mu_{\mathrm{Tot}}^{-1} = \sum_i \mu_i^{-1}, \quad (1)$$

TABLE II. Theoretical expressions for mobilities calculated through this work. $k_B$: Boltzmann constant; $T$: temperature; $\mathscr{F}_{1/2}$: Fermi integral; $\hbar = h/2\pi$: Planck constant; $e$: electronic charge; $K_S$: static dielectric constant; $K_d$: optical dielectric constant; $m^*$: effective mass; $\rho$: material density; $u_l$: sound velocity; $L$: screening length; $E_{1c}$: acoustic deformation potential; $\theta$: optical phonon Debye temperature; $w$: longitudinal optical mode frequency; $\Omega$: $a^3/4$: unit cell volume; $a$: lattice constant; $\epsilon$: reduced energy; and $F$: reduced Fermi level.

| | | |
|---|---|---|
| Ionized impurity | $\mu_{ii} = \dfrac{4K_S^2(k_BT)^{3/2}}{3\pi\sqrt{2}e^3(m^*)^{1/2}N_i\mathscr{F}_{1/2}f(b)} I$<br>$I = \int_0^\infty \dfrac{\epsilon^3 \exp(\epsilon - F)}{[\exp(\epsilon - F) + 1]^2} d\epsilon$<br>$f(b) = \ln(1+b) - b/(b+1)$<br>$b = 32\pi^2 m^* k_{B_0} TL^2 \bar{\epsilon}/h^2$ | (Ref. 16) |
| Acoustic phonon | $\mu_{PA} = \dfrac{2(2\pi)^{1/2} e\hbar^4 \rho u_l^2}{3(m^*)^{5/2}E_{1c}^2(k_BT)^{3/2}}$ | (Ref. 17) |
| Polar optical phonon | $\mu_{PO} = \dfrac{16\hbar K_0(2\pi k_BT)^{1/2}}{(3ewm^*/m_0)^{3/2}} \dfrac{K_SK_d}{K_S - K_d} J$<br>$J = [\exp(\theta/T) - 1]G(\theta/T)$<br>$G(\theta/T) = 1$, when $\theta/T \ll 1$<br>$G(\theta/T) = \frac{3}{8}(\pi\theta/T)^{1/2}$, when $\theta/T \gg 1$ | (Ref. 18) |
| Alloy scattering | $\mu_A = (2e/3m^*\mathscr{F}_{1/2})H$<br>$H = \int_0^\infty \dfrac{\tau_A \epsilon^{3/2} \exp(\epsilon - F)}{\exp(\epsilon - F) + 1} d\epsilon$<br>$\tau_A = \dfrac{32\hbar^4 \epsilon^{-1/2}}{3\sqrt{2}\pi(\Delta U)^2(m^*)^{3/2}(k_BT)^{1/2}\Omega}$ | |

where $\mu_{\mathrm{Tot}}$ is the resulting mobility and $\mu_i$ is the mobility due to a specific kind of scattering mechanism.

In order to visualize which mechanisms predominate in the entire range of temperatures studied, we utilized Eq. (1) with the known expressions for mobilities (Table II[16-18]) as well as the known parameters for InGaAsP.

In Fig. 3, this calculated mobility is shown as a function of the reciprocal of absolute temperature, between 4.2 and 300 K, for $n = 5.0 \times 10^{17}$ cm$^{-3}$, the total ionized impurity concentration $N_i = 7.0 \times 10^{17}$ cm$^{-3}$ and the alloy scattering potential $\Delta U = 0.5$ eV. From this figure we observe the following results: (a) The acoustic phonon scattering does not

TABLE I. Experimental results for the four samples.

| Sample | $n$ ($\times 10^{16}$ cm$^{-3}$) $T = 4.2$ K | $n$ ($\times 10^{16}$ cm$^{-3}$) $T = 300$ K | $\mu_H$ ($\times 10^3$ cm$^2$/V s) $T = 4.2$ K | $\mu_H$ ($\times 10^3$ cm$^2$/V s) $T = 300$ K | $d$ ($\mu$m) |
|---|---|---|---|---|---|
| MF161 | 1.6 | 2.02 | 2.92 | 2.46 | 0.55 |
| MF162 | 2.6 | 4.20 | 3.02 | 2.19 | 0.60 |
| MF139 | 52 | 51.0 | 1.41 | 1.51 | 0.55 |
| MF138 | 160 | 179 | 2.61 | 2.75 | 0.55 |



[This article is copyrighted as indicated in the article. Reuse of AIP content is subject to the terms at: http://scitation.aip.org/termsconditions. Downloaded to ] IP: 143.106.108.133 On: Tue, 25 Nov 2014 18:41:19

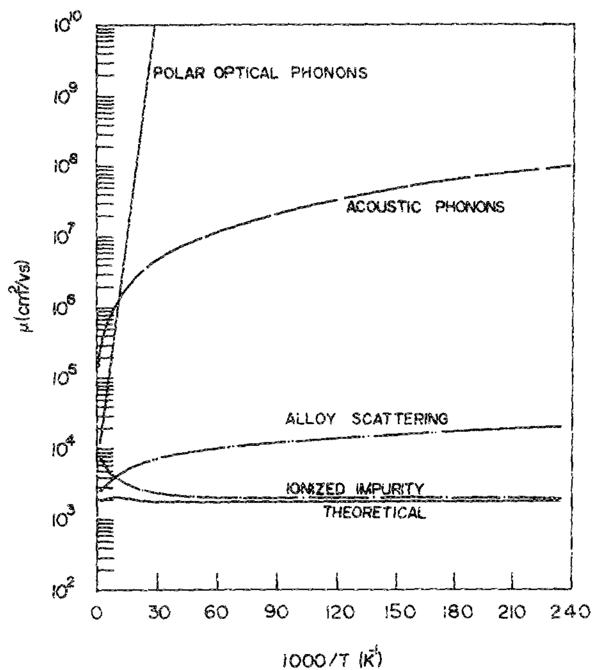


FIG. 3. Theoretical mobility vs $10^3/T$ for $n = 5.0\times10^{17}$ cm$^{-3}$ and $N_i = 7.0\times10^{17}$ cm$^{-3}$.

have a significant influence in the calculation of the total mobility over the range of temperatures studied. (b) At room temperatures, the polar optical phonons and alloy scatterings are the predominant scattering mechanisms. (c) At low temperature, both the ionized impurity and alloy scattering are dominant. Therefore, for InGaAsP, ionized impurity scattering is not the only important scattering mechanism at low temperature (4.2 K).

In order to analyze the experimental results, we have to calculate the alloy scattering potential ($\Delta U$), which appears in the alloy scattering mobility expression, and the total ionized impurity concentration ($N_i$), which appears in the ionized impurity mobility expression.

All other physical constants are known or estimated by[13]

$$Q(x,y) = \{x(1-x)\,[(1-y)\,T_{12}(x) + yT_{43}(x)] + y(1-y)\,[(1-x)T_{14}(y) + xT_{23}(y)]\} \times [x(1-x) + y(1-y)]^{-1},$$

where $T_{ij}$ is the material parameter for the ternary alloy formed by binaries $i$ and $j$.

We start by taking $N_i$ that gives the theoretical mobility limited by ionized impurity equal to experimental value found at 4.2 K. Of course, by the analysis above we know that this is not good for samples with lower carrier concentrations. However, with this $N_i$, we calculated $\Delta U$ for the best fit (by using the least-square technique) between 4.2 and 300 K. Now, with this value of $\Delta U$, we use $N_i$ as a variable parameter to find the optimum value of $N_i$ which gives the best fit to the experimental curve. Taking this new value of $N_i$, the curve fitting process is repeated to find a new value of $\Delta U$, etc. Thus, with this iterative method we were able to fit the experimental curves, as can be seen in Fig. 4.

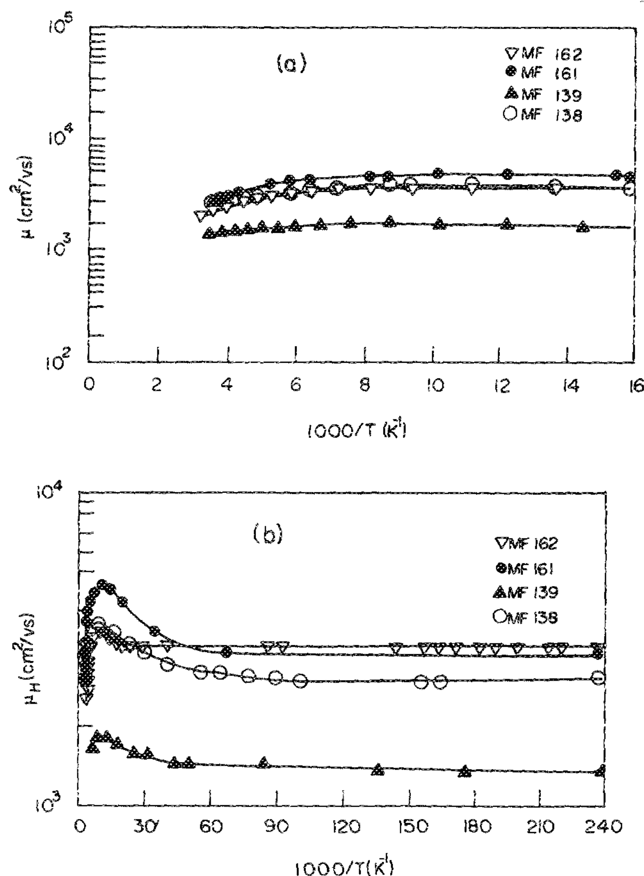


FIG. 4. (a) The line is the theoretical curve, and the points are the experimental data of the mobility vs $10^3/T$ between 65 K and room temperature. (b) The line is the theoretical curve, and the points are the experimental data of the mobility vs $10^3/T$ between 4.2 K and room temperature.

Table III shows the experimental results for $\Delta U$ and $N_i$ for each sample. The theoretical values of $\Delta U$ shown in Table III, were calculated following the equation[19]

$$(\Delta U)^2 = x(1-x)y^2(\Delta U_{ABD})^2 + x(1-x)\,(1-y)^2\,(\Delta U_{ABC})^2 + y(1-y)x^2(\Delta U_{BCD})^2 + y(1-y)(1-x)^2(\Delta U_{ACD})^2, \quad (2)$$

where $\Delta U_{ABC}$ is the ternary scattering potential of the $A_{1-x}B_xC$ compound, that assumes different values depending on the theory used.

It is important to mention that Eq. (1) was modified to

TABLE III. Experimental and theoretical values of $\Delta U$. $N_i$ is the total ionized impurity concentration.

| Sample | $N_i$ ($\times10^{16}$ cm$^{-3}$) | $\Delta U$ (eV) (experimental) | $\Delta U$ (eV) (theoretical) |
|---|---|---|---|
| MF161 | 1.88 | 0.56 | BGD = 0.52 |
| MF162 | 4.65 | 0.61 | EAD = 0.39 |
| MF139 | 68.6 | 0.52 | END = 0.37 |
| MF138 | 507 | 0.62 | |



[This article is copyrighted as indicated in the article. Reuse of AIP content is subject to the terms at: http://scitation.aip.org/termsconditions. Downloaded to ] IP: 143.106.108.133 On: Tue, 25 Nov 2014 18:41:19

$$\frac{1}{\mu_H} = \frac{1}{r_1 \mu_1} + \frac{1}{r_2 \mu_2} + \frac{1}{r_3 \mu_3} + \frac{1}{r_4 \mu_4}, \tag{3}$$

where $r_1$, $r_2$, $r_3$, and $r_4$ were calculated from the usual expression $r_i = \langle \tau_i \rangle^2 / \langle \tau_i \rangle^2$ for each scattering mechanism.

In order to calculate $\langle \tau \rangle$, $\langle \tau^2 \rangle$, $\mu_1$, $\mu_2$, $\mu_3$, and $\mu_4$, we need the Fermi-level energy which was calculated from[20]

$$n = N_c \mathscr{F}_{1/2} (\eta_F), \tag{4}$$

where $N_c$ represents the effective density-of-states in the conduction band, $\mathscr{F}_{1/2}$ is the Fermi integral,[21] and $\eta_F$ is the reduced Fermi-level energy.

## IV. DISCUSSION

For calculating the Fermi-level position, we have assumed that $n_H = r/eR_H$, where $e$ is the electron charge and $r$ is the Hall factor. For our material, the value of $r$ is between 0.98 and 1.03.[13] This allows us to take $r = 1$ as a good approximation.

The calculated Fermi level showed that Boltzmann statistics were not adequate to describe electrons in our samples. In fact, at low temperatures ($T < 30$ K) all samples were degenerate.

The Brooks–Herring formula for ionized impurity scattering, as well as all others formulas, were modified in order to take into account the Fermi–Dirac statistics. This gives a higher value of calculated mobility limited by ionized impurity scattering at low temperatures than the same mobility calculated by Boltzmann statistics. As a consequence, as can be seen in Fig. 3, mobility limited by alloy scattering can be comparable to mobility limited by ionized impurity.

## V. CONCLUSION

We have performed transport measurements in InGaAsP ($E_g = 0.96$ eV) taking into account the Fermi-Dirac statistics and the low-temperature mobility. The values found for the alloy scattering potential $\Delta U$ agree much better with the BGD theory than the other theories. The value found for $\Delta U$ in our work is significantly smaller than the $\Delta U = 0.8$ eV found by Bhattacharya *et al.*[13] even though their theoretical curves fit very well with their experimental results. We think the reason for this difference is their use of Boltzmann statistics, which gives a lower value of mobility limited by ionized impurity scattering, and so in order to have a good fit of experimental values, they needed a higher value of $\Delta U$. A lower value of $\Delta U$, closer to that found by us and predicted by the BGD theory, would be found if the correct statistics were used to fit their experimental curves.

Further improvements in our method could be achieved by taking the tail of density-of-states function and nonparabolic effects for heavier doped samples.


## ACKNOWLEDGMENTS

We wish to thank Dr. F. C. Prince who provided us with the samples used in this work, as well as Dr. N. B. Patel for the helpful discussions and suggestions, and to A. C. Franco da Silveira, who helped us with computer calculations.



[1] F. C. Prince, N. B. Patel, S. Chang, and D. J. Bull, IEEE J. Quantum Electron. **QE-17**, 597 (1981).
[2] F. Capasso, R. A. Logan, P. W. Foy, and S. Sumski, Electron. Lett. **16**, 241 (1980).
[3] P. K. Bhattacharya and M. D. Yeaman, Solid-State Electron. **24**, 297 (1981).
[4] J. W. Harrison and J. R. Hauser, J. Appl. Phys. **47**, 292 (1976).
[5] M. Glicksman, R. E. Enstrom, S. A. Mittleman, and J. R. Appert, Phys. Rev. B **9**, 1621 (1974).
[6] J. J. Tietjen and L. R. Weisberg, Appl. Phys. Lett. **7**, 261 (1965).
[7] T. Makowski and M. Glicksman, J. Phys. Chem. Solids **34**, 487 (1973).
[8] Y. Takeda, A. Sasaki, Y. Imamura, and T. Takagi, J. Appl. Phys. **47**, 5405 (1976).
[9] J. W. Harrison and J. R. Hauser, Phys. Rev. B **13**, 5347 (1976).
[10] J. R. Hauser, M. A. Littlejohn, and T. H. Glisson, Appl. Phys. Lett. **28**, 458 (1976).
[11] M. A. Littlejohn, J. R. Hauser, and T. H. Glisson, Appl. Phys. Lett. **30**, 242 (1977).
[12] J. C. Phillips, Rev. Mod. Phys. **42**, 317 (1970).
[13] P. K. Bhattacharya, J. E. Ku, S. J. T. Owen, G. H. Olsen, and S. H. Chiao, IEEE J. Quantum Electron. **QE-17**, 150 (1981).
[14] P. D. Greene, S. A. Wheeler, A. R. Adams, A. N. El-Sabbahy, and C. N. Ahmad, Appl. Phys. Lett. **35**, 78 (1979).
[15] T. P. Pearsall, Electron. Lett. **17**, 169 (1981).
[16] A. C. Beer, *Solid State Physics*, Suppl.4 (Academic, New York, 1963).
[17] J. D. Wiley, in *Semiconductors and Semimetals*, edited by R. K. Willardson and A. C. Beer (Academic, New York, 1975), Vol. 10, p. 127.
[18] D. J. Howarth and E. H. Sondherimer, Proc. R. Soc. London A **219**, 53 (1953).
[19] M. A. Littlejohn, J. R. Hauser, T. H. Glisson, D. K. Ferry, and J. W. Harrison, Solid-State Electron. **21**, 107 (1978).
[20] J. S. Blakemore, *Semiconductor Statistics* (Pergamon, New York, 1962), p. 117.
[21] V. I. Fistul, *Heavily Doped Semiconductors* (Plenum, New York, 1969), p. 369.





[This article is copyrighted as indicated in the article. Reuse of AIP content is subject to the terms at: http://scitation.aip.org/termsconditions. Downloaded to ] IP: 143.106.108.133 On: Tue, 25 Nov 2014 18:41:19